

Available online at www.sciencedirect.com**ScienceDirect**journal homepage: <http://www.elsevier.com/locate/rpor>**Original research article****MC safe bunker designing for an 18 MV linac with nanoparticles included primary barriers and effect of the nanoparticles on the shielding aspects****Amir Ghasemi-Jangjoo^{a,b}, Hosein Ghiasi^{a,*}**^a Tabriz University of Medical Sciences, Medical Radiation Research Team, Tabriz, Iran^b Tabriz University of Medical Sciences, Radiation Therapy and Oncology Department, Tabriz, Iran**ARTICLE INFO****Article history:**

Received 7 July 2017

Received in revised form

12 December 2018

Accepted 9 May 2019

Available online 6 June 2019

Keywords:

Shielding

Monte Carlo simulation

Nanoparticles

Radiotherapy

ABSTRACT

Aim: The aim of this study was to design a safe bunker for an 18 MV linac in to configuration; primary barriers made from nanoparticle-containing concrete and pure concrete.

Background: Application of some nanoparticles in the shielding materials has been studied and it was shown that the presence of some nanoparticles improved radiation shielding properties.

Materials and methods: Some percentage of different nanoparticles were modeled by the MCNP5 code of MC in the megavoltage radiotherapy treatment room's primary barriers. Other parts of the designed room, such as secondary barriers and maze door, were modeled as ordinary pure concrete. A safe bunker was designed according to the MC derived spectra at primary and secondary barriers location using a modeled and benchmarked 18 MV linac in free air. Then, the thickness of the required shielding materials for the door and also concrete for the walls and primary barriers were calculated separately.

Results: According to the results, required concrete thickness in primary and secondary barriers was reduced by around 0.8% compared to pure concrete application. Additionally, required lead and BPE decreased by 25% and 15%, respectively, due to primary barriers nanoparticles.

Conclusions: It was concluded that application of some nanoparticles in the shielding materials structures in megavoltage radiotherapy can make the shielding effective.

© 2019 Greater Poland Cancer Centre. Published by Elsevier B.V. All rights reserved.

1. Background

Recently developed megavoltage radiotherapy electron linear accelerators (linacs) have offered some important advantages

as compared to low energy machines. These include skin sparing effect, low scattering and mostly forward photon beam irradiation in radiotherapy which has made it possible to deliverer the prescribed dose to deep-seated tumors without damage to superficial and surrounding normal tissues.^{1–11} Although these may seem to be important advantages of megavoltage linacs, radiation contamination inside the room and around the linac may be considered as a cost for the above mentioned advantages.^{4–9} Although the main electron

* Corresponding author.

E-mail address: hoseinghiasi62@gmail.com (H. Ghiasi).

<https://doi.org/10.1016/j.rpor.2019.05.009>

1507-1367/© 2019 Greater Poland Cancer Centre. Published by Elsevier B.V. All rights reserved.

and photon beam presence is in field and out of field at the patient couch,¹² photoneutron and, consequently, prompt capture gamma ray propagate in any direction. Isotropic^{19,20} propagation pattern has been reported for photoneutrons contaminating almost anywhere that the photoneutrons get on the wall or low Z material and, consequently, energetic capture gamma ray is produced. Radiation contamination in the megavoltage radiotherapy may cause secondary malignancies.^{3–9} Then, at a bunker with inadequate shielding, in addition to the patient undergoing megavoltage radiation therapy, the staff may also receive additional dose equivalent to the neutron and gamma ray. According to the International Commission on Radiological Protection (ICRP) report 103, radiation dose can be expressed as the ratio of mean energy deposited in the unit of the absorbed matter.¹⁴

Conversion of dose to dose equivalent which is more relative to biological effects of the radiation needs the radiation weighting factor to be applied in the calculations. For electron and photon in all energies, the factor, ω_R , is recommended as 1 but it was reported energy dependent for neutrons. Dose equivalent is calculated from below equation.

$$H_T = \sum_R \omega_R D_{R,T} \quad (1)$$

where H_T is dose equivalent in tissue T from radiation R.

According to Table B.3 of ICRP annals publication 2007,¹³ ω_R for neutrons is as follows.

- (a) $E < 10 \text{ KeV}$; $\omega_R = 5$
- (b) $10 \text{ KeV} < E < 100 \text{ KeV}$; $\omega_R = 10$
- (c) $100 \text{ KeV} < E < 2000 \text{ KeV}$; $\omega_R = 20$
- (d) $2000 \text{ KeV} < E < 20,000 \text{ KeV}$; $\omega_R = 10$
- (e) $E > 20,000 \text{ KeV}$; $\omega_R = 5$

According to the literature and reported results of studies on the photoneutron spectra produced in medical linacs,¹⁴ photoneutrons energy reaches up to 3 MeV with mean energy of 1.5 MeV around the linac and 100–200 KeV at the maze and maze entrance. The neutrons energies can mainly be categorized in c where $\omega_R = 20$ at the maze entrance of treatment room, which may be dangerous and lead to secondary malignancies. Shielding against the above mentioned radiation contaminations is necessary and, on the other hand, optimum shielding requires a proper shielding material. Concrete has been reported as a good shielding material. Recently, the use of nanotechnology and addition of some nanoparticles in a concrete composition has been reported to increase the attenuation factor in the photon and neutron radiation fields. Monte Carlo (MC) simulation was used to the concrete photon linear and mass attenuation factor; μ in (cm^{-1}) and μ/p in ($\text{cm}^2 \text{ g}^{-1}$), and also neutron linear and mass removal cross-section Σ_R in (cm^{-1}) and $\sum R/\rho$ in ($\text{cm}^2 \text{ g}^{-1}$) in the presence of and without nanoparticles. Then, a safe bunker designed by MC simulation and analytical methods which compared between nanoparticle-containing primary barriers and those of pure concrete. A safe bunker was modeled and discussed in our previous work with pure concrete with the same methods.

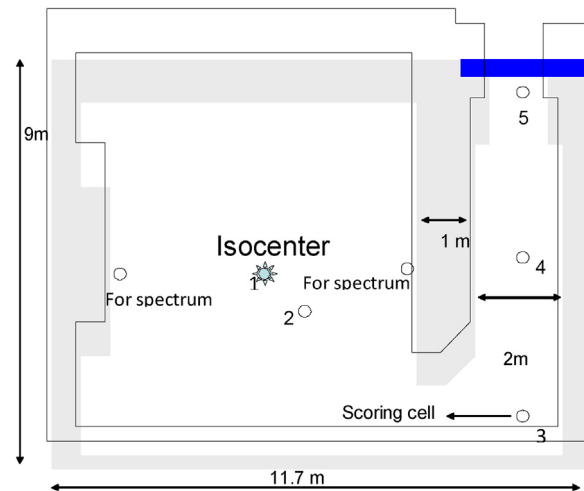


Fig. 1 – The schematic representation of the room geometry used in the current study simulated by Monte Carlo simulation.

2. Aim

The aim of this study was to design a safe bunker for 18MV linac in to configuration; primary barriers made from nanoparticle-containing concrete and pure concrete. Our aim was to apply nanoparticles in the megavoltage shielding to reduce the required thickness of shielding materials.

3. Materials and methods

In the current study, MC simulation and analytical methods were used to investigate the effect of the presence of nanoparticles in a concrete composition on the photon and neutron linear and mass attenuation factors. The MCNP5 code of MC, the International Atomic energy Agency (IAEA) safety report 47,¹⁵ and the National Council on Radiation Protection and Measurements (NCRP) report 151¹⁶ recommended analytical methods used in this work. To design a safe bunker with nanoparticle-containing concrete for a treatment room (shown in Fig. 1) including an 18MV Varian 2100Clinac irradiation, the linac was modeled precisely and according to the measured values benchmarked and verified. The method and explanation of the modeled linac and benchmarking process was according to our previous works.¹⁸ Verification and benchmarking the modeled linac for the photoneutron calculations conducted by the calculation of apparent neutron source strength (Q_N which shows the number of photoneutrons production by linac per X-ray Gy at isocenter) calculation for the linac and comparison with the reported value literatures. Q_N has been defined by IAEA no. 47¹⁶ and NCRP no. 151¹⁷ as “the number of neutrons produced by linac per Gy of X-ray delivering to the isocentre in n/Gy X-ray of the isocentre. An 18MV Varian 2100Clinac was simulated and considered for the calculations. Photon and neutron spectra were derived at the primary barriers. Required thickness of nanoparticle-containing concrete was calculated to reduce the radiation to dose limit; photon and neutron. The formulations

recommended by the IAEA safety report 47 and NCRP report no. 151^{16,17} were used. Neutron and photon dose equivalent were also obtained at the maze entrance. The ordinary wall concrete composition as recommended by the NCRP report no.144¹⁹ contains 1.5% B₄C, 1.5% WO₃ and 1.5% Fe₂O₃ and 1.5% PbO₂. The micro-scale lattice configuration was considered to fill the walls materials with the nano-scale particles. 1.5% per g (weight percent in concrete) in the voxel simulated walls were simulated and the nano-particles were simulated in 20 nm diameter and spherical shape. The nano-spheres filled the walls simulated by the lattice configuration with 0.1 mm cubic voxels. All of the room walls were simulated in a lattice configuration with 0.1 mm cubic voxels filled by the 20 nm nanoparticles. Radiation attenuation, fluence and dose variation caused by the presence of the nano-scale materials were evaluated by comparing the parameters with a room made of ordinary pure concrete. An overview on the above mentioned attenuation factors is made below for more clarification.

$$I(x) = I_0 e^{-\mu x} \quad (2)$$

$I(x)$ is the transmitted and scored photons or gamma ray intensity (in the modeled good geometry) while I_0 is the radiation initial intensity. μ and x are the linear attenuation factors in cm⁻¹ and cm, respectively. By dividing the linear attenuation factor (μ) by density, the mass attenuation factor in cm² g⁻¹ is obtained as in below equation.

$$\frac{\mu}{\rho} = \frac{1}{\rho x} \ln \left(\frac{I_0}{I} \right) \quad (3)$$

Neutron macroscopic removal cross-section and mass removal cross-section are obtained from the below equations; where A is the atomic mass number, σ_t is the total interactions cross-section and Z in Eq. (6) is the effective atomic number.

$$\sum R(\text{cm}^{-1}) = \frac{0.602\rho}{A} \sigma_t \quad (4)$$

$$\sum \frac{R}{\rho} = 0.206A^{-1/3}Z^{-0.294}(\text{cm}^2 \text{g}^{-1}) \quad (5)$$

Thickness of the required shielding material is recommended to be calculated from the below equations.

Number of required tenth value layers of shielding materials equals to

$$\text{No of TVLS} = \log_{10} \left(\frac{1}{B} \right) \quad (6)$$

In the above equation, the required attenuation of barrier B may be determined according to a desired dose constraint (design limit) that is derived from an occupational or public dose limit.

3.1. Monte Carlo simulation

MCNP5 is a MC code was developed in 2007 by the Los-Alamos National Library (LANL) and has been widely used for the radiological problems. Different studies have been conducted using the MCNPX code and interesting, useful and helpful

results were reported in radiology and radiotherapy physics as well as shielding design. An 18MV Varian 2100Clinac was simulated fully. The main simulated parts of the linac were the target, electron stopper, primary collimator, movable jaws, flattening filter, complex and massive lead shielding and secondary collimator, and other fine parts. The modeled linac was verified and benchmarked using the comparison of measured and simulated percent depth dose (PDD) and photon beam profile (PBP) dataset at the depth of 103.3 cm (Isocentre) from the target in a 50 cm × 50 cm × 50 cm water phantom. PDD and PBP dataset were consistent with our previous work. Photon and photoneutron spectra and dose derived at the primary and secondary barriers and the derived spectra were used as the source in the concrete attenuation factor calculation. After room designing, photoneutron and neutron capture gamma ray spectra as well as linac leakage X-ray spectra and dose were derived at the maze entrance. Linear attenuation factor and mass attenuation factor for derived energy spectra was used to calculate primary barrier concrete, door lead and borate polyethylene (BPE) thickness.

3.2. Analytical methods

IAEA no. 47 and NCRP no. 151^{15,16} recommended the formulation proposed by Wu and McGinley²³ to calculate neutron and prompt gamma ray dose equivalent at the maze entrance. Both methods are based on the neutron fluence at the inner maze entrance, Q_N and dimensions of the room. Additionally, for linac leakage photon dose calculation at the maze entrance, the reports recommended a formulation. Our dose calculation by the analytical methods in this study is based on the methods recommended by IAEA no. 47 and NCRP no. 151 as well as the used factors value. Explanation of the methods is as follows.^{16,17}

Neutron spectra from the linac at the isocenter were shown in Fig. 2 which were derived by Monte Carlo simulation. Neutron fluence at the inner maze entrance, maze entrance neutron and gamma ray dose equivalent were calculated using Eqs. (7), (8) and (9), respectively.

$$\varphi_A = \frac{Q_N}{4\pi d^2} + \frac{5.4Q_N}{2\pi S} + \frac{1.26Q_N}{2\pi S} \quad (7)$$

$$D_n = 2.4 \times 10^{-15} \times \varphi_A \times \sqrt{\frac{A_r}{S_1} \times (1.64 \times 10^{-d_2/1.9} + 10^{-d_2/T_N})} \quad (8)$$

where T_N obtained from and S_1 is the cross-section of the maze in m². Capture gamma ray dose equivalent for straight maze is calculated from the below equation.

$$D_\varphi = 5.7 \times 10^{-16} \times \varphi_A \times 10^{-d_2/6.2} \quad (9)$$

The reader can find explanation of the parameters in equations 8–10 in the IAEA safety report no. 47, NCRP report no. 151 and Wu-McGinley 2003 paper.^{16,17,20} Equations 9 and 10 were proposed by Wu-McGinley and recommended by the mentioned protocols. Then, the number of required TVLs was calculated for obtained total radiation dose shielding according to the protocols recommendations.

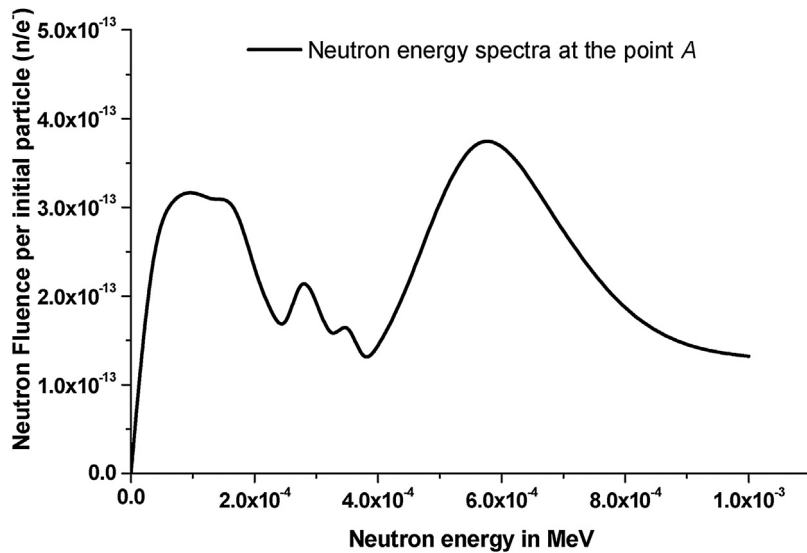


Fig. 2 – Photoneutron spectra derived by Monte Carlo simulation at the isocenter of the studied 18 MV linac.

Table 1 – Neutron dose estimation at different locations in and out of the bunker using both Monte Carlo simulation and analytical method.

Point	Mean analytical results in mSv Gy^{-1}	Dose equivalent mSv Gy^{-1}	Mean analytical results in mSv Gy^{-1} this study	Dose equivalent (mSv Gy^{-1}) in this study
1(isocentre)	6.90×10^{-1}	5.41×10^{-1}	6.20×10^{-1}	5.45×10^{-1}
2	3.10×10^{-1}	2.67×10^{-1}	3.65×10^{-1}	2.77×10^{-1}
3	9.60×10^{-2}	8.54×10^{-2}	9.12×10^{-2}	8.50×10^{-2}
4	8.54×10^{-3}	6.74×10^{-3}	8.39×10^{-3}	7.71×10^{-3}
5(50 cm inner the door)	3.16×10^{-3}	2.16×10^{-3}	3.90×10^{-3}	1.56×10^{-3}
6(50 cm outer the door)	n/a	n/a	2.89×10^{-3}	9.65×10^{-5}

4. Results

In the current study, MC simulation and analytical methods were used to calculate photon and neutron dose equivalent at the primary and secondary barriers as well as the maze entrance. MC simulation results showed that the neutron fluence at the isocentre without walls in the regular field sizes of $10\text{ cm} \times 10\text{ cm}$, $20\text{ cm} \times 20\text{ cm}$, $40\text{ cm} \times 40\text{ cm}$ was $9.01 \times 10^{-9} \text{ n/cm}^2$, $8.43 \times 10^{-9} \text{ n/cm}^2$ and $7.81 \times 10^{-9} \text{ n/cm}^2$. Photon dose equivalent at the isocentre was 0.12×10^{-15} per primary electron. Then, 8.33×10^{14} primary electrons were required to run to deliver 1 X-ray Gy dose equivalent to the isocentre and for this electron incidence on the target, 1.34×10^{12} neutrons were produced. From calculations, our simulated linac model neutron source strength (Q_N) was 1.34×10^{12} neutrons per Gy of X-ray at the isocentre. The obtained factor is an essential value for the neutron dose equivalent calculation by MC simulation because the simulation results are the value per primary source photon or particle. According to the MC neutron dose calculation and because $10\text{ cm} \times 10\text{ cm}$ is recommended as a standard field size, photoneutron dose equivalent at 3.3 m and 3.6 m from the isocentre (primary and secondary barriers positions, respectively) were obtained by MC simulation as $1.5 \times 10^{-2} \text{ Sv/Gy}$ X isocentre and $1.2 \times 10^{-2} \text{ Sv/Gy}$ X isocentre, respectively. On

the other hand, photon dose obtained as $9.25 \times 10^{-2} \text{ Gy/Gy}$ of X-ray at the isocentre. Table 1 shows the neutron dose estimation at different locations of the simulated room. At the secondary barrier position, only scattered, leakage X-ray and other photons dose were found to be much lower than the primary barrier location. To calculate the required thickness of concrete for designing a secondary barrier, the public area factor was applied and the $840 \times 10^{-3} \text{ m}$ obtained while the same value for nanoparticles was $834 \times 10^{-3} \text{ m}$. MC simulation method calculated the TVL for the ordinary concrete and above mentioned nanoparticles included ordinary concrete for the 18MV photon spectrum as $4443 \times 10^{-3} \text{ m}$ and $4403 \times 10^{-3} \text{ m}$ respectively. For five days a week (8 h per working day), the workload recommended as 600 Gy and inserting the value in the recommended formulation for design dose limit calculation for the control area, required concrete thickness for the primary barrier obtained as $1779 \times 10^{-3} \text{ m}$ and $1765 \times 10^{-3} \text{ m}$ for the pure and nanoparticle-containing ordinary concretes. Secondary barrier should shield the scattered, leakage and other X-ray in the linac housing. MC derived photon and neutron spectra at the primary and secondary barriers were used to calculate the required thickness (TVLs numbers) to design a safe bunker. At the maze entrance, prompt gamma ray, leakage X-ray and photoneutron spectra were used to model a narrow beam source in a good

geometry to obtain required BPE and lead thickness to a maze entrance door. The obtained thickness was 9 mm lead (in two layers of 4.5 mm in a sandwich configuration) and 34 mm BPE. Because the recommended analytical methods are insensitive to nanoparticle-containing concrete, the calculations made separately and results were compared with the differences of the MC simulation results discussed. In our previous work,¹⁷ a safe bunker for an 18MV Varian 2100 C/D linac was designed using MC simulation and new released protocols recommendation on the photon and photoneutron shielding design for megavoltage linacs. In the previous work,¹⁷ we calculated thickness and TVL for ordinary pure concrete. But in this paper nanoparticle-containing concrete was applied to model the primary barriers. According to the results, using nanoparticles in the primary barrier modeling led to around 0.8% decrease in the required thickness for the primary barriers as compared to pure concrete. Additionally, in case of the maze door, a 25% reduction in lead thickness and 25% in the required thickness of BPE was obtained in the presence of nanoparticles in the primary barrier in comparison to pure and nanoparticle-containing primary barriers. Also, it can be said that a 0.7% reduction in the required secondary barriers was obtained due to the application of nanoparticles in the primary barriers. Results of our previous work showed that without recommendation and based on the linac produced photon and neutron dose and spectra; it is possible to design a safe bunker with low difference with the analytical methods proposed in recommendations. In the current study, our aim was to use the same procedure but difference between this work and our previous work was that in the current study, the primary barriers of the designed treatment room was modeled as a nanoparticle-containing ordinary concrete. Designing a room with primary barriers with nanoparticle-containing concrete reduced the required thickness, TVL as well as maze entrance radiation contamination dose equivalent. This led to a decrease in the thickness of maze door shielding; lead and BPE. Around 4–7% decrease was shown in the photon and neutron mass attenuation factors in nanoparticle-containing ordinary concrete. According to the results, the required thickness of nanoparticle-containing ordinary concrete for the primary barriers, lead in door design and BPE as door shielding material decreased. Additionally, dose from photoneutrons, prompt gamma ray and leakage photons from the modeled linac showed a decrease through the application of primary barriers with nanoparticles. Comparing our previous work¹⁸ in which the primary barriers were modeled as ordinary concrete and results of this work were nanoparticles were applied in the primary barriers concrete composition, revealed that nanoparticles decreased dose and shielding thickness from 0.7% for secondary barriers to 25% for lead and 15% for the required thickness of BPE. Our considered door was in a sandwich configuration and performed well in this study. Additionally, good agreement was revealed between MC simulation and the methods reported in protocols. Differences may be attributed to the fact that analytical calculations cannot take into account the effect of nanoparticles in the radiation removal. Finally, it should be stated that the increase of around 8% in the concrete shielding properties

reported by Mesbahi and Ghiasi²⁴ is in good agreement with this study results.

5. Conclusion

We modeled a megavoltage radiotherapy treatment room walls made of ordinary concrete loaded with some percentage of different nano-scale particles in the primary barriers. The results showed an increasing attenuation factor in the concrete loaded with nanoparticles. Consequently, the primary barriers made of concrete containing nanoparticles led to lower concrete requirement for the barriers design. It was revealed that the shielding properties of ordinary concrete loaded with nanoparticles was enhanced. Further studies and more precise investigation are recommended to obtain more results.

Conflict of interest

None declared.

Financial disclosure

None declared.

Uncited references

21–23.

REFERENCES

- Konefal A, Orlef A, Bieniasiewicz M. Measurements of neutron radiation and induced radioactivity for the new medical linear accelerator, the Varian TrueBeam. *Radiat Meas* 2016;86:8–15.
- Janiszewska M, Polaczek-Grelak M, Raczkowski K, Szafron B, Konefal A, Zipper W. Secondary radiation dose during high-energy total body irradiation. *Strahlenther Onkol* 2014;190(5):459–66.
- Konefal A, Orlef A, Laciak M, Ciba A, Szewczuk M. Thermal and resonance neutrons generated by various electron and X-ray therapeutic beams from medical linacs installed in polish oncological centers. *Rep Pract Oncol Radiother* 2012;17(July & LPKT;6&RPKT;):339–46.
- Kelleter L, Wroncka A, Besuglow J, et al. Spectroscopic study of prompt-gamma emission for range verification in proton therapy. *Phys Med* 2017;34:7–17.
- Konefal A, Laciak M, Dawidowska A, Osewski W. Significant change in the construction of a door to a room with slowed down neutron field by means of commonly used inexpensive protective materials. *Radiat Prot Dosimetry* 2014;162(December & LPKT;3&RPKT;):197–207.
- Mesbahi A, Ghiasi H. Shielding properties of the ordinary concrete loaded with micro- and nano-particles against neutron and gamma radiations. *Appl Radiat Isot* 2018;136:27–31.
- Polaczek-Grelak K, Karaczyń B, Konefal A. Nuclear reactions in linear medical accelerators and their exposure consequences. *Appl Radiat Isot* 2012;70(October & LPKT;10&RPKT;):2332–9.

8. Konefal A, Orlef A, Dybek M, Maniakowski Z, Polaczek-Greluk K, Zipper W. Correlation between radioactivity induced inside the treatment room and the undesirable thermal/resonance neutron radiation produced by linac. *Phys Med* 2008;24(December &LPKT;4&RPKT;):212–8.
9. Konefal A, Polaczek-Greluk K, Zipper W. Undesirable nuclear reactions and induced radioactivity as a result of the use of the high-energy therapeutic beams generated by medical linacs. *Radiat Prot Dosimetry* 2008;128(2):133–45.
10. Ghiasi H, Mesbahi A. Monte Carlo characterization of photoneutrons in the radiation therapy with high energy photons: a comparison between simplified and full Monte Carlo models. *Iran J Radiat Res* 2010;8:187–93.
11. Ghiasi H. Monte Carlo characterizations mapping of the &LPKT; γ ; &TDREFS; n &RPKT; and &LPKT; n , γ &RPKT; &TDREFS; photonuclear reactions in the high energy X-ray radiation therapy. *Rep Pract Oncol Radiother* 2014;19:30–6.
12. Mesbahi A, Ghiasi H, Mahdavi SR. Photoneutron and capture gamma dose calculations for a radiotherapy room made of high density concrete. *Nucl Tech Radiat Protec* 2011;26(2):147–52.
13. Ghiasi H, Mesbahi A. Sensitization of the analytical methods for photoneutron calculations to the wall concrete composition in radiation therapy. *Radiat Meas* 2012;47:461–4.
14. International Commission on Radiological Protection &LPKT;ICRP&RPKT;. The 2007 recommendations of the International Commission on Radiological Protection. ICRP No. 103 Report. 2007.
15. Al-Affan IA. Estimation of the dose at the maze entrance for X-rays from radiotherapy linear accelerators. *Med Phys* 2000;27(1):231–8.
16. International Atomic Energy Agency &LPKT;IAEA&RPKT;. Radiation protection in the design of radiotherapy facilities. Safety reports series no. 47. &LPKT;GENERIC&RPKT; Ref Type: Report. Vienna: IAEA; 2006.
17. National Council on Radiation Protection and Measurements &LPKT;NCRP&RPKT;. Structural shielding design and evaluation for megavoltage X-ray and gamma-ray radiotherapy facilities. NCRP No. 151. 2005. p. 1–246.
18. Beigi M, Afarande F, Ghiasi H. Safe bunker designing for the 18 MV Varian 2100 Clinac: a comparison between Monte Carlo simulation based upon data and new protocol recommendations. *Rep Pract Oncol Radiother* 2016;21(1):42–9.
19. National Council on Radiation Protection and Measurements &LPKT;NCRP&RPKT;. Radiation protection for particle accelerator facilities. NCRP Report No. 144. 2005. p. 1–512.
20. Mesbahi A, Ghiasi H, Mahdavi SR. Photoneutron and capture gamma dose equivalent for different room and maze layouts in radiation therapy. *Radiat Prot Dosimetry* 2010;140:242–9.
21. Ghiasi H, Mesbahi A. A new analytical formula for neutron captures gamma dose calculations in double-bend mazes in radiation therapy. *Rep Pract Oncol Radiother* 2012;17(4):220–5.
22. Waller EJ, Jamieson TJ, Cole D, Cousins T, Jammal RB. Experimental and computational determination of neutron dose equivalent around radiotherapy accelerators. *Radiat Prot Dosimetry* 2003;107(4):225–32.
23. Wu RK, McGinley PH. Neutron and capture gamma along the mazes of linear accelerator vaults. *J Appl Clin Med Phys* 2003;4:162–71.
24. Mesbahi A, Ghiasi H. Shielding properties of the ordinary concrete loaded with micro- and nano-particles against neutron and gamma radiations. *Appl Radiat Isot* 2018;136(June):27–31.